Design of a Beam Dump for the TTF-FEL Phase II (TTF2) Project

The modification of the existing TESLA Test Facility dump

M. Maslov [1], A. Lokhovitskii [1], M. Schmitz[2]

[1] IHEP Protvino, Russia; [2] DESY Hamburg, Germany

Design of a Beam Dump for the TTF-FEL Phase II (TTF2) Project

The modification of the existing TESLA Test Facility dump

M. Maslov [1), A. Lokhovitskii [1), M. Schmitz [2)

[1) IHEP Protvino, Russia; [2) DESY Hamburg, Germany

1 Introduction and Requirements

The existing TESLA Test Facility phase 1, so called TTF1, will stop its operation by the end of the year 2002. After that the test facility will be extended in terms of energy, to make further

Parameter	TTF2	TTF1
E_0, beam energy	$\leq 2\text{GeV}$	$\leq 0.8\text{GeV}$
I_{ave}, average beam current	$\leq 64\mu\text{A}$	
N_t, number of particles per bunch train	$\leq 4\cdot10^{13}$ electrons	
ν_t, repetition rate of bunch trains	$\leq 10\text{Hz}$	
T_t, length of bunch train	$\leq 800\mu\text{s}$	
$\sigma_x\cdot\sigma_y$, spot size of beam at dump entrance	$\geq 1\text{mm}^2$	$\geq 2.5\text{mm}^2$
W_t, energy carried in one bunch train	$\leq 13\text{kJ}$	$\leq 5.1\text{kJ}$
P_{ave}, average beam power	$\leq 130\text{kW}$	$\leq 51\text{kW}$

Table 1.1: Main beam parameters of TTF2 in comparison with TTF1

accelerator related studies (e.g. cavity gradient, beam diagnostics, …) for TESLA and will deliver Free Electron Laser (FEL) radiation into a dedicated experimental hall. The main parameters of this second phase of the TESLA Test Facility, TTF2, are listed in table 1.1 and compared to those of TTF1.

This report deals with the design of a beam dump for TTF2. In particular it investigates by what kind of modifications the existing TTF1 beam dump [1] may be applied for TTF2 operation. This is a reasonable approach, since the TTF2 requirements differ from TTF1 in energy and average power only by a factor of 2.5. In addition two spare TTF1-type beam dumps exist, which were formerly installed in the S-Band test facility, but are hardly activated and can therefore be used for modification.
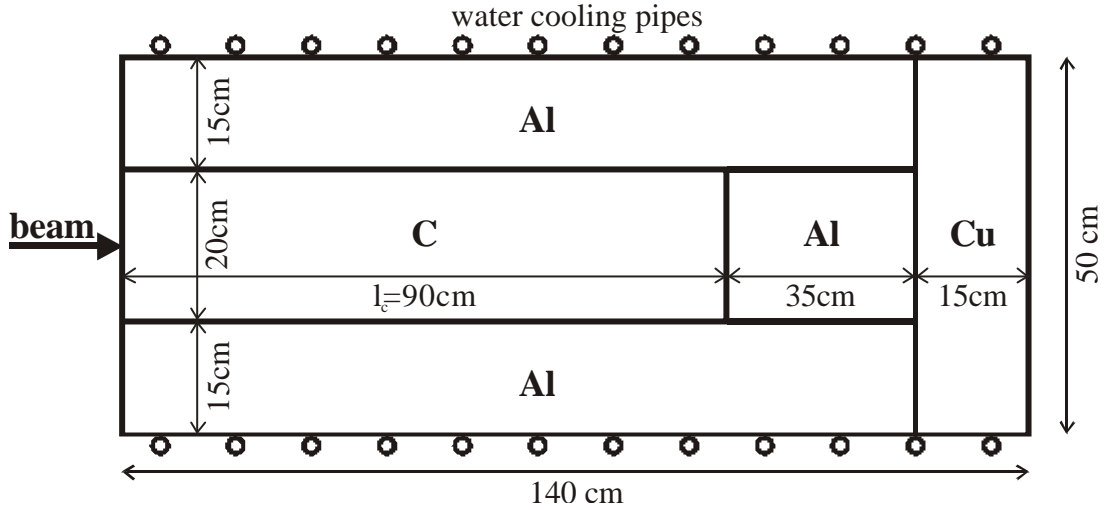
Figure 1.1: Side view of the cylindrical geometry of the TTF1 beam dump

Figure 1.1 shows the geometry of the TTF1 beam dump. It consists of a cylindrical graphite core with a length of l_c=90cm, which is shrink-fitted into an aluminum tube. At the downstream end aluminum and copper are introduced to absorb the tail of the shower and to minimize the total absorber length. The 35cm long aluminum core is also shrink-fitted into the surrounding aluminum tube like the graphite part. The dump operates at the surrounding atmosphere and is edge cooled at its circumference by copper cooling pipes. As valid for this dump, the requirements for the TTF2 dump can be expressed in a similar way, namely:

1. Withstand the beam parameters as given in table 1.1, i.e. absorption of 13kJ energy per bunch train in combination with 130kW average beam power. The beam spot size at the dump entrance is assumed to be $\sigma_x \cdot \sigma_y \geq 1mm^2$.

2. The energy absorption efficiency should be more than 99%.

3. The volume for the dump block should not exceed $1m^2$ in cross section and 2m in length.

4. Since the absorber is exposed to normal atmosphere, the maximum temperature in graphite should not exceed 450-500°C in order to prevent its oxidization.

5. As follows from the mechanical properties of aluminum, its temperature should stay below 200-250°C.

The next section shortly recalls the fundamental equations, which are necessary when dealing with radiation heating in solid absorbers. By means of the shower simulation code MARS [2], which gives the distribution of the deposited energy in the dump, analytical estimations of the dump heating are presented in section 3. The limits of the TTF1 dump, when operated at TTF2 parameters, are shown and possible variants of modification by means of adding a front part of the same radial C-Al structure and introducing a slow beam sweeping or using one or more graphite spoilers upstream of the dump are discussed. After having chosen for one of the modification variants in section 4, section 5 evaluates the temperature and mechanical stress distribution of this variant in more detail by using the finite element code ANSYS. At the end of this report the proposed modification of the TTF1 dump, which will finally be applied at TTF2, is shortly summarized.

2   Fundamentals on Dump Heating

In general the temperature distribution T(r,z,t) within a cylindrical absorber is obtained as the solution of the heat equation:

$$\frac{\partial}{\partial t}T(r,z,t) = \frac{\lambda}{\rho \cdot c} \cdot \nabla^2 T(r,z,t) + \frac{1}{\rho \cdot c} \cdot Q(r,z,t)$$

where ρ is the mass density, c the specific heat and λ the heat conductivity of the material. The boundary and initial conditions have to be set according to the specific problem. The heat source Q(r,z,t) describes how much power is deposited per unit of volume. Neglecting the bunch structure, the heat source is constant in time over the period of the bunch train and zero at any other time, i.e.:

$$Q(r,z,t) = \begin{cases} N_t \cdot \varepsilon(r,z)/T_t & \text{for} \quad \frac{n}{\nu_t} \le t \le \frac{n}{\nu_t} + T_t \quad ;n = 0,1,2,3,4,\dots \\ 0 & \text{for} \quad \text{any other time} \end{cases}$$

$\varepsilon(r,z)$ is the energy deposition per unit of volume induced by one primary electron impinging on the absorber. This value is determined by Monte Carlo simulation of the electromagnetic shower (EMS). A complete solution of the heat equation is possible only numerically, e.g. by using the finite element code ANSYS [3] as done in section 5.

Nevertheless some analytical estimation can be done if the problem is split up into instantaneous heating during one bunch train and average heating, which assumes that the beam current is not pulsed but constant in time with the amplitude I_{ave}. The characteristic thermal diffusion length $L = \sqrt{(\lambda \cdot T_t)/(\rho \cdot c)}$ during the bunch train passage time T_t=0.8ms is about 0.25mm in graphite or copper. This is small compared to the beam size and therefore we assume, that the temperature rise ΔT_{inst} caused by one bunch train passage is directly proportional to the distribution of deposited energy, i.e.:

$$\Delta T_{inst}(r,z) = \frac{\varepsilon(r,z) \cdot N_t}{\rho \cdot c} \qquad \textit{Equation 2.1}$$

A conservative estimate of the maximum temperature T_{max} in the absorber is:

$$T_{max} \le T_0 + \Delta T_{inst}(r = 0) + \Delta T_{eq}(r = 0) \qquad \textit{Equation 2.2}$$

where T_0 is the temperature of the heat sink, which is in our case the cooling water at the circumference of the absorber with an outer radius of R and ΔT_{eq} is the solution of the heat equation in the stationary case, i.e. $\frac{\partial}{\partial t}T(r,z,t) = 0$ and $Q(r,z) = N_t \cdot \nu_t \cdot \varepsilon(r,z)$. With such a heat source and if only radial heat flow is assumed, we obtain from the stationary heat equation:

$$N_t \cdot \nu_t \cdot \varepsilon(r,z) = -\lambda \cdot \frac{1}{r}\frac{\partial}{\partial r}r\frac{\partial}{\partial r}\Delta T_{eq}(r,z)$$

$$\Leftrightarrow \quad \Delta T_{eq}(r,z) = \frac{N_t \cdot \nu_t}{\lambda} \cdot \int_{s=r}^{R} \frac{ds}{s} \cdot \int_{u=0}^{s} \varepsilon(u,z) \cdot u \cdot du \qquad \textit{Equation 2.3}$$

Equation 2.3 may be either integrated numerically or by using an empirical fit-function for $\varepsilon(r,z)$. If the so called Grindhammer paramatrization [4] is used:

$$\varepsilon(r,z) = \frac{dE(z)}{dz} \cdot \frac{2 \cdot \sigma^2(z)}{\pi \cdot \left(r^2 + 2 \cdot \sigma^2(z)\right)^2} \qquad \text{with} \qquad \frac{dE(z)}{dz} = \int_{r=0}^{R} \varepsilon(r,z) \cdot 2\pi r \cdot dr$$

equation 2.2 can be written as:

$$T_{max} \leq T_0 + \frac{dE(z)}{dz} \cdot \frac{N_t}{\pi} \cdot \left[\frac{1}{\rho \cdot c \cdot 2 \cdot \sigma^2(z)} + \frac{\nu_t}{4 \cdot \lambda} \cdot \ln\left(1 + \frac{R^2}{2 \cdot \sigma^2(z)}\right) \right] \qquad \textit{Equation 2.4}$$

where $dE(z)/dz$ is the radially integrated energy deposition per unit length of the absorber and per one primary electron, R is the outer radius of the absorber and $\sigma(z)$ is the radial rms-width of the deposited energy in the dump at the longitudinal position z. Therefore at the dump entrance (z=0) $\sigma(0)$ is identical to the beam size, but inside the absorber (z>0) $\sigma(z)$ depends on both, the size of the incoming beam and the radial shower development.

With the knowledge as presented above the heating of a given cylindrical solid dump geometry can be estimated. In any case an EMS simulation code has to be used to get $\varepsilon(r,z)$ or the fit-parameter $\sigma(z)$ for the Grindhammer parametrization.

3   Estimation of Dump Heating for different Modification Variants

Different variants of modifying the TTF1 dump (see figure 1.1) in order to deal with the TTF2 parameters are compared in this section in terms of heating. Estimation on instantaneous (ΔT_{inst}) and equilibrium (ΔT_{eq}) heating are derived from equation 2.1 and 2.3, where $\varepsilon(r,z)$ is taken from the output of the EMS simulation code MARS. Although the specific heat and the thermal conductivity are a function of temperature (see table 5.1 and 5.2), they are in this section assumed to be constant. Since the specific heat of graphite increases with temperature, a value of 0.68J/(g·K), which is valid for room temperature, was chosen. The thermal conductivity of graphite decreases with temperature. Therefore the value of 0.75W/(cm·K), which is true at a 500K to 700K operation temperature, was chosen. In the case of aluminum, specific heat as well as thermal conductivity go up with temperature. Therefore the values at room temperature were used, i.e. 0.86J/(g·K) for the specific heat and 1.7W/(cm·K) for the thermal conductivity. In that sense the results of the following estimations can be regarded as being quite conservative.

First of all it was investigated how the existing TTF1 dump, as shown in figure 1.1, behaves when it is exposed to the TTF2 operation parameters, i.e. $E_0=2GeV$, $N_t=4 \cdot 10^{13}e^-$, $\nu_t=10Hz$, $\sigma_x \cdot \sigma_y=1mm^2$. The resulting instantaneous temperature rise ΔT_{inst} after the passage of one bunch train as well as the sum of instantaneous and equilibrium heating $\Delta T=\Delta T_{inst}+\Delta T_{eq}$ along the absorber are shown in figure 3.1. It can easily be seen, that the tolerable temperature limits for graphite (500°C) and aluminum (250°C), as postulated in section 1, are exceeded by far, since the maximum temperature of graphite resp. aluminum will rise by about 630K resp. 420K.

This situation can be relaxed if the beam is slowly swept along a circular line with radius r_{slow} at the face of the dump. In that case the radial heat flow in the dump starts from a larger inner radius. Thus the equilibrium temperature drop ΔT_{eq} is reduced. The distribution of instantaneous heating is not affected by slow sweeping, since the bunch train passage time is very short compared to the slow sweeping period. For a slow beam sweeping with $r_{slow}=2cm$ the resulting ΔT_{eq} as well as $\Delta T=\Delta T_{inst}+\Delta T_{eq}$ are also shown in figure 3.1. The maximum temperature rise in the graphite section of the TTF1 dump is now pushed down to a tolerable value of about 420K, whereas the aluminum part still operates at a too high value of around $\Delta T=340K$. Table 3.1 gives the maximum temperature rise $\Delta T=\Delta T_{inst}+\Delta T_{eq}$ in the graphite and aluminum section for other values of slow sweep radii.
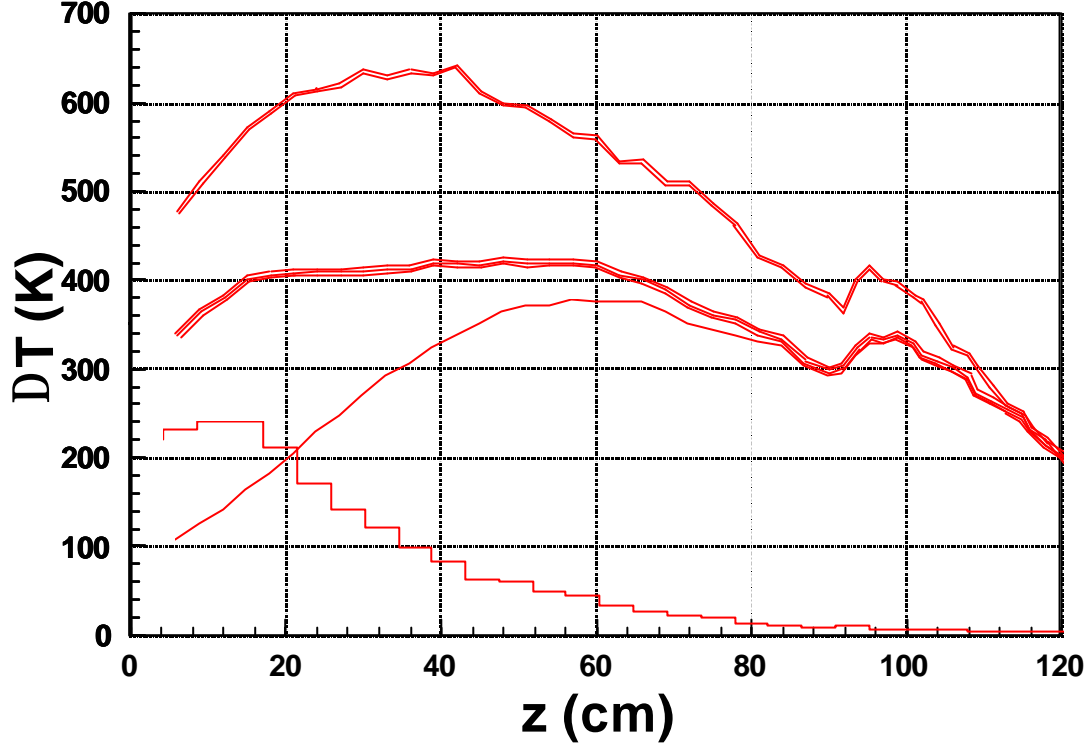
Figure 3.1: Maximum temperature rise along the TTF1 dump when operated with TTF2 beam parameters, i.e. E_0=2GeV, N_t=4·10^{13}e⁻, ν_t=10Hz, $\sigma_x \cdot \sigma_y$=1mm². Solid step line shows instantaneous heating ΔT_{inst} induced by one bunch train. The sum of instantaneous and equilibrium heating $\Delta T = \Delta T_{inst} + \Delta T_{eq}$ is displayed without any slow sweeping (double solid line) and when slow sweeping with r_{slow}=2cm is applied (triple solid line). For the latter case ΔT_{eq} is also shown (single solid line).

Even at r_{slow}=5cm the temperature rise in the aluminum section is just at the limit for a safe long term operation, without any safety margin. It has to be mentioned, that all estimations on the equilibrium temperature rise are a result of equation 2.3. Temperature drops due to the thermal resistance across the boundaries at r=10cm from graphite respectively aluminum core to the surrounding aluminum and from the absorber to the water cooling have been neglected so far. A further increase of the slow sweep radius beyond r_{slow}=5cm seems to be unreasonable, because the graphite core of the dump has only a radius of 10cm. Therefore even without any beam position fluctuations the remaining radial margin to the surrounding aluminum would be only half a Molière

r_{slow}	$(\Delta T)_{max}=(\Delta T_{inst}+\Delta T_{eq})_{max}$	
	in graphite section	in aluminum section
0 cm	630 K	420 K
1 cm	500 K	370 K
3 cm	360 K	300 K
5 cm	280 K	240 K

Table 3.1: Maximum temperature rise $(\Delta T)_{max}=(\Delta T_{inst}+\Delta T_{eq})_{max}$ in the graphite and aluminum section of the TTF1 dump, when operated at TTF2 parameters for different slow sweep radii r_{slow}.

length of graphite section, l_c	beam energy, E_0	C-section		Al-section		Cu-section	
		$(dE/dz)_{max}$ [MeV/cm]	$(dP/dz)_{max}$ [W/cm]	$(dE/dz)_{max}$ [MeV/cm]	$(dP/dz)_{max}$ [W/cm]	$(dE/dz)_{max}$ [MeV/cm]	$(dP/dz)_{max}$ [W/cm]
90 cm	800 MeV	8.2	530	7.2	470	8.9	580
90 cm	2 GeV	16	1040	24	1560	38	2470
110 cm	2 GeV	16	1040	19	1290	28	1820
130 cm	2 GeV	16	1040	13	850	18	1170

Table 3.2: Maximum of thermal loading for different parts of the dump at I_{ave}=64µA and different length l_c of the graphite section.

length. In addition to that, there is another argument, why this simple solution of taking the unchanged TTF1 dump in combination with a slow sweeping system is not acceptable. The energy leakage of the TTF1 dump at 2GeV operation is more than 1%. Extending the dumps front part by, using the same radial graphite aluminum composition, will reduce the heating of the subsequent aluminum and copper section as well as the energy leakage.

For an average beam current of 64µA table 3.2 lists the maximum values for the energy resp. power depositions $(dE/dz)_{max}$ resp. $(dP/dz)_{max}$ in the different sections (graphite, aluminum, copper) of the dump. In graphite the maximum energy deposition is located at the shower maximum, which is at $z\approx$60cm for 2GeV and at $z\approx$40cm for 800MeV. 1MeV/cm of dE/dz corresponds to 64W/cm of dP/dz, since $dP/dz=I_{ave}/e\cdot dE/dz$ and I_{ave}=64µA. Without any modification of the TTF1 dump, where
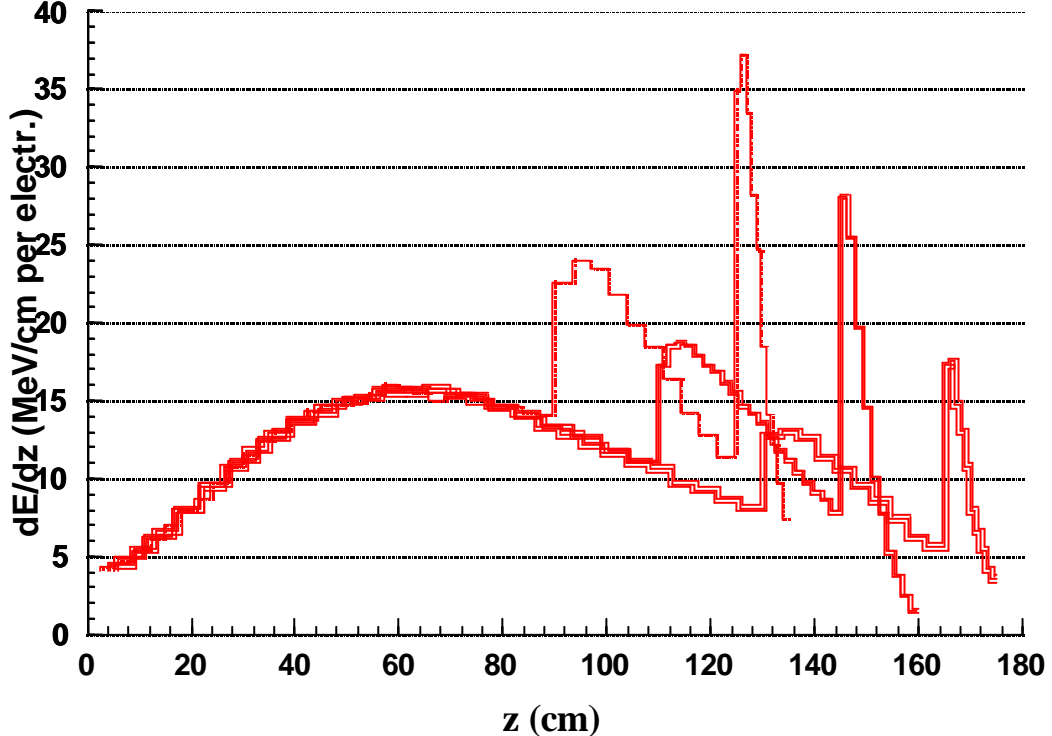

Figure 3.2: Longitudinal distribution of deposited energy dE/dz per unit length and per one incident electron at 2GeV/64µA operation. Single solid line represents the unmodified TTF1 dump with l_c=90cm. Situation with extended front part of l_c=110cm is shown as double solid line and triple solid line l_c=130cm.

the length of the graphite section is l_c=90cm, the power density increases by a factor of 2 in the graphite section, more than a factor of 3 in the aluminum section and more than a factor of 4 in the copper section, when the dump is operated at 2GeV instead of 800MeV.

If the front part is extended by 40cm, i.e. l_c=130cm, the maximum power depositions in the aluminum and copper sections can be reduced by a factor of 2 compared with the unmodified TTF1 dump. In that case $(dP/dz)_{max}$ is at a similar level of about 1kW/cm in all 3 sections of the dump. The longitudinal profile of dE/dz at 2GeV/64μA operation is shown in figure 3.2 for the unmodified TTF1 dump l_c=90cm and two different extensions l_c=110cm and l_c=130cm.

The resulting maximum temperature rise $\Delta T = \Delta T_{inst} + \Delta T_{eq}$ along the modified TTF1 dump with a 40cm front part extension, i.e. l_c=130cm, when operated at TTF2 parameters in combination with a slow beam sweeping of r_{slow}=2cm is shown in figure 3.3. The situation in the graphite section is of course identical to the case l_c=90cm, i.e. ΔT=420K, but in the aluminum section the temperature rise is now drastically reduced to a safe value of ΔT=180K.

To determine the maximum absolute temperature in the dump, the temperature of the heat sink, namely the cooling water, and the temperature drops across the graphite to aluminum boundary at r=10cm as well as the aluminum-aluminum boundary at r=10cm and due to the heat transfer from the dump surface into the cooling water at r=25cm have to be taken into account. According to table 3.2 the maximum thermal loading in the graphite and aluminum section is at the level of 1kW/cm. Assuming a reasonable heat transfer coefficient of 0.2W/(cm^2·K) [5] at the mentioned boundaries, will result in a maximum temperature drop of about 80K at the graphite-aluminum as well as the aluminum-aluminum boundary at r=10cm and 30K at the dump to cooling water boundary. If the cooling water flow is 1kg/s, the difference of the water temperature between forward and return pipe will be 30K at P_{ave}=130kW. At a forward cooling water temperature of 30°C the average
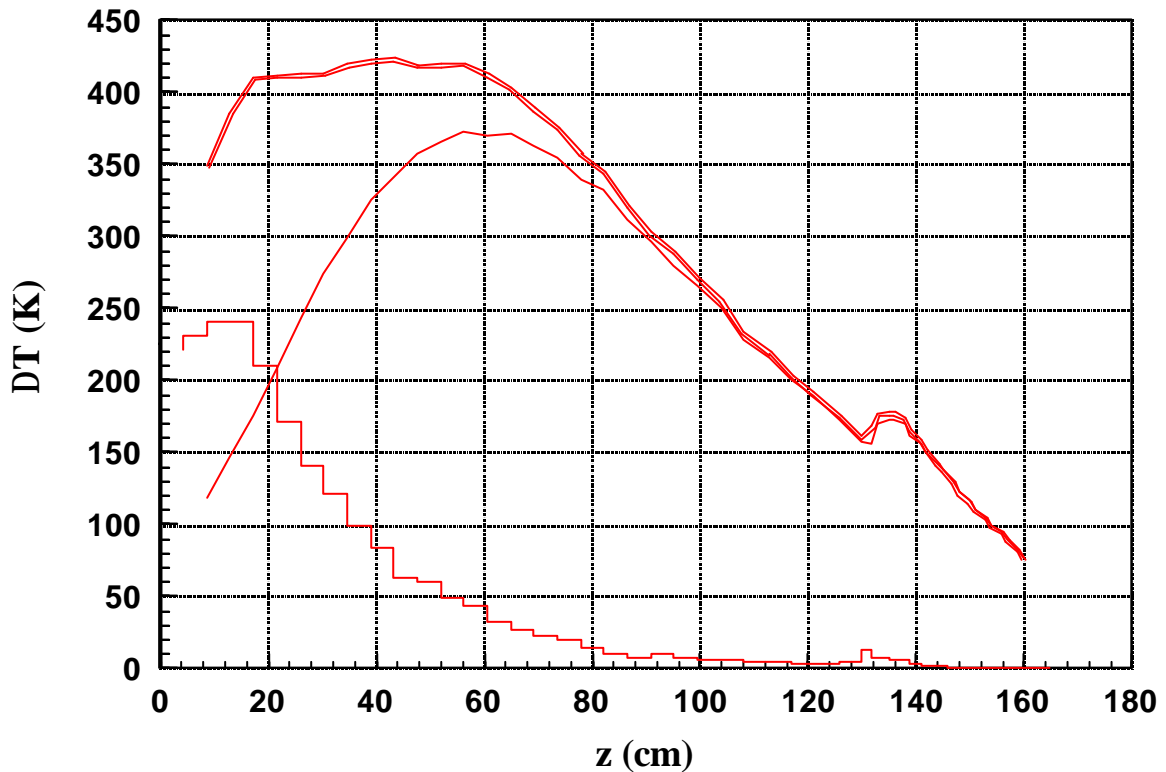

Figure 3.3: Maximum instantaneous heating ΔT_{inst} (solid step line), max. equilibrium heating ΔT_{eq} (single solid line) and the sum of both (double solid line) along the modified TTF1 dump with a 40cm front part extension, i.e. l_c=130cm, when operated at TTF2 parameters in combination with a slow beam sweeping of r_{slow}=2cm.

	sweeping radius	sweeping period	amplitude of integrated magnetic field for each plane	remarks
slow sweeping system	$r_{slow} = 2cm$	$\tau_{slow} \leq 2s$	± 0.07 Tm	
fast sweeping system	$r_{fast} = 1mm$	$\tau_{fast} \leq 0.8ms$, pulsed with ν_t	± 0.004 Tm	necessary if beam size << 1mm^2

Table 3.3: Main parameters of a slow and fast sweeping system, which is located 2m upstream of the dump face, for a 2GeV/c beam in Variant A.

temperature of the heat sink can be set to $T_0=45°C$.

Therefore in combination with the information of figure 3.3 the absolute maximum temperature in graphite will be about 45°C+420K+80K+30K=575°C. Since this is really at the limit for graphite operation under air, special attention has to be paid for a good thermal contact between graphite and the surrounding aluminum. The maximum temperature in the aluminum section behind the graphite part can be estimated similarly to about 45°C+170K+80K+30K=325°C, which is already slightly exceeding the tolerable limit. But as mentioned at the beginning, this is only a rough and rather conservative estimate. For a more detailed numerical analysis see section 5.

As has been worked out up to here this modification of the existing TTF1 dump is a possible solution for TTF2 application. It is called Variant A and sketched in figure 3.5. The existing TTF1 dump is extended by a 40cm long front part with the same radial graphite-aluminum geometry and a slow beam sweeping with a sweep radius of $r_{slow}=2cm$ has to be applied. In order to achieve a good thermal contact, as mentioned above, the 40cm extension part will be made of two graphite parts with a conical outer shape and two aluminum parts with a similar conical inner shape. Pulling the two aluminum parts together and therefore pressing them onto the graphite surface guarantees a good thermal contact. The existing TTF1 dump was manufactured by shrink-fitting the graphite cylinder into the aluminum. This method is more complicated, since it requires high precision machining of the outer diameter of the graphite core as well as the inner diameter of the aluminum cylinder.

The 40cm extension reduces power deposition and thus heating of the aluminum and copper sections behind the graphite section. It also pushes the total energy absorption of the dump beyond the 99% level. Slow beam sweeping is required to reduce the equilibrium temperature rise mainly in the graphite section.

Circular beam sweeping is achieved by two orthogonal deflecting systems (dipoles), which are excited in a sine- and cosine-like way with the same frequency and amplitude to produce a circular deflection. To provide a homogeneous heat distribution, the period of the slow sweeping system $\tau_{slow}=1/\nu_{slow}$ must be significantly shorter (3-4 times) than the characteristic time of thermal diffusion within the limits of the sweep radius. For graphite and $r_{slow}=2cm$ the characteristic thermal time constant gives $c \cdot \rho \cdot r_{slow}^2/\lambda \approx 8s$ and thus $\tau_{slow} \approx 2-3s$. Instantaneous heating is not affected by slow sweeping, since the bunch train passage time $T_t << \tau_{slow}$. Instantaneous heating depends on the beam spot size at the dump entrance. If this will be essentially less than $\sigma_x \cdot \sigma_y = 1mm^2$, as presently assumed, ΔT_{inst} as shown in figure 3.3 will increase its maximum far beyond the present 250K value. In that case a fast beam sweeping system with $\tau_{fast}=T_t$ and a sweeping radius of $r_{fast} \approx 1mm$ has to be introduced additionally to distribute the electrons within the time of a bunch train passage. This would be a system, pulsed with the repetition rate ν_t of bunch trains. Under the assumption that the sweeping system is separated from the dump face by a 2m drift space, table 3.3 summarizes the main parameters of the required deflection system for a 2GeV/c beam.

Instead of using a slow beam sweeping system, the power density in the graphite section of the dump can be reduced by application of a spoiler. This solution is shown as variant B in figure 3.5. To experience only ionization losses with negligible shower development, the spoiler thickness should be less than 30% of the radiation length, which gives 7.5cm of graphite. The graphite spoiler has to be located about 2m upstream of the dump. The dump in this variant consists of the existing TTF1 dump modified by a 32.5cm front part extension. Together with the spoiler, the added graphite part in front of the TTF1 dump has a total length of 40cm as in variant A. The temperature rise $\Delta T = \Delta T_{inst} + \Delta T_{eq}$ for variant B is shown as dotted line in figure 3.4. The spoiler temperature increases by about 430K and the maximum temperature rise in the graphite section of the dump is at about the same level. It appears about 50cm downstream of the dump entrance.

A third solution, called variant C and sketched in figure 3.5, does also work without a slow sweeping system. It uses a distributed set of 3 graphite spoilers, which have an increasing thickness of 5cm, 10cm and 25cm. The first and second spoiler are interspaced by 100cm, the second and the third by 35cm and the third spoiler is finally located 30cm upstream of the dump. In this variant C the existing TTF1 dump can remain completely unchanged. Therefore again the total length of additional graphite in front of the TTF1 dump is 40cm as in the other variants A and B. The temperature rise for variant C can be seen as solid line in figure 3.4. The first spoiler is of course exposed similar to that in variant B. The subsequent spoilers increase in temperature by about 270K and 340K. The graphite of the TTF1 dump reaches a maximum of 380K roughly 30cm downstream of the dump's face.

It has to be mentioned, that as well as in variant A also for variant B and C a fast sweeping system is necessary, if the beam spot at the first spoiler is smaller than 1mm^2.
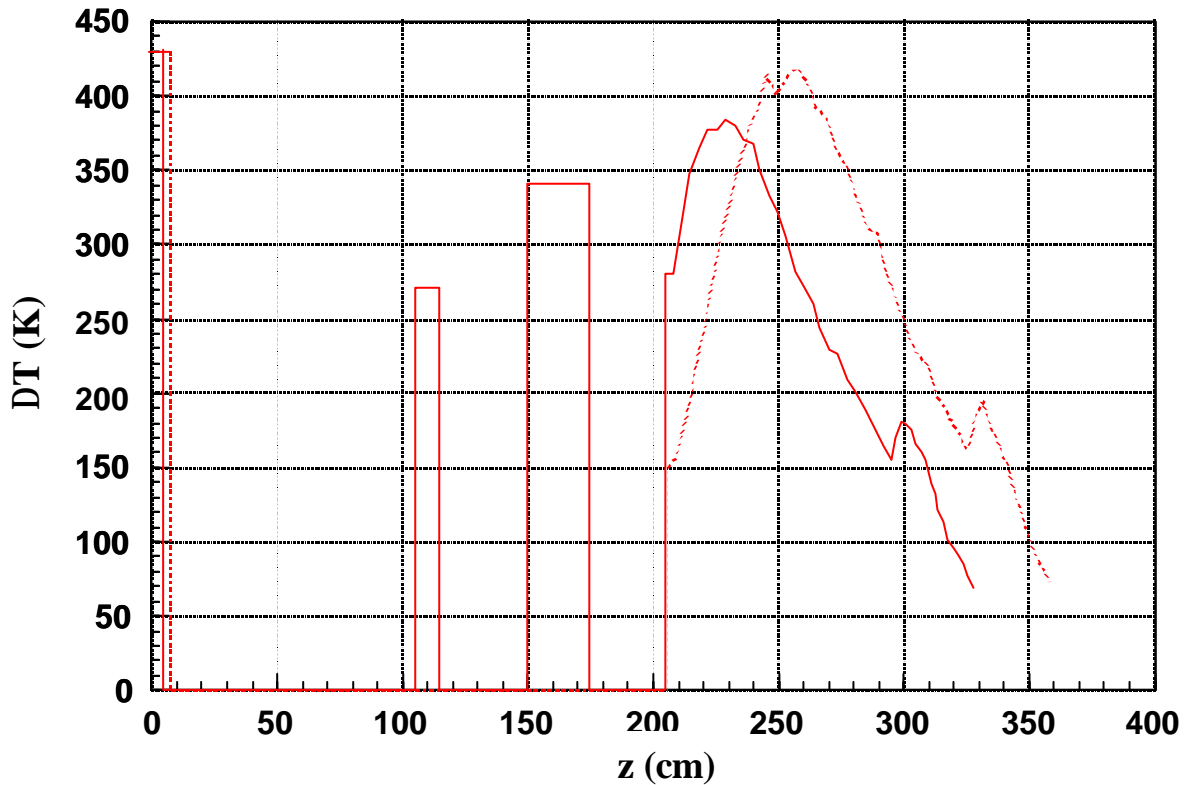

Figure 3.4: Maximum temperature rise $\Delta T = \Delta T_{inst} + \Delta T_{eq}$ for variant B (dotted line) and variant C (solid line).
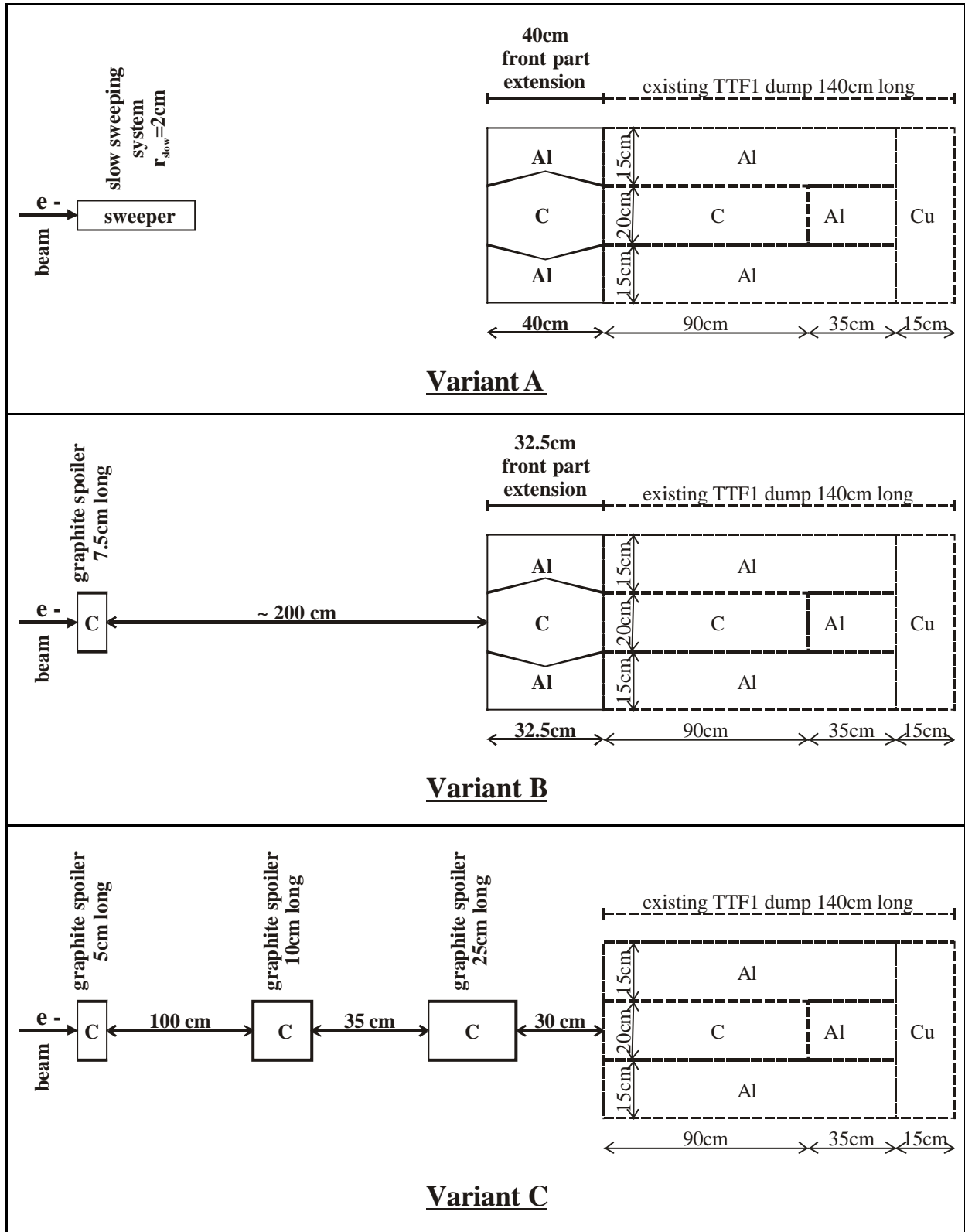
Figure 3.5: Overview of the possible modification variants A, B and C for the existing TTF1 dump, in order to make it applicable for TTF2 operation.

4   Discussion on Choice of preferred Modification Variant

Three possible schemes for a TTF2 dump, by incorporating the existing TTF1 dump were presented in the previous section. Variant B and C have the advantage of being totally passive. Nevertheless for reasons of air activation, the spoiler system has to be installed in the vacuum pipe. Since the dump is operated at normal atmosphere, an exit window for the beam is required in any variant just in front of the dump face. Each spoiler has to be cooled and will also be a location of activation. Therefore activation is not concentrated at the position of the dump, but somehow distributed.

For these reasons the spoiler solutions variant B and C are not as simple as they promised to be at first sight. In addition the beam line to the dump is quite short, so the most compact and simple scheme must be chosen.

Therefore variant A is the preferred solution for TTF2.

5   Temperature and Mechanical Stress Analysis of selected Variant by means of ANSYS code

The preferred variant A will be studied in more detail concerning its temperatures and the resulting mechanical stresses in the material. The ANSYS code Version 4.4 has been used for this purpose. The geometry is sketched in figure 5.1, but the copper part was not included in the ANSYS calculations. At the beginning the whole dump is at a temperature of 300K, which is determined by the temperature T_0 of the heat sink, namely the cooling water, at the outer cylindrical surface of the dump. According to the result from the EMS simulation, each bunch train deposits a certain amount of energy in every volume element of the dump. As a consequence the temperature in this volume element increases instantaneously. In the time up to the next bunch train, this temperature decays according to thermal diffusion, i.e. heat conduction towards the heat sink. At the beginning the temperature right after a bunch train passage increases from train to train. This process of heating up the "cold" dump, starting at T_0=300K, is demonstrated in figure 5.2 for the beginning of the aluminum section at z=130cm in its center at r=0cm and near the circumference at r=25cm. In this figure the temperatures are still increasing from train to train, but after a while the temperature $T(t,x,y,z)$ at a given time t and position (x,y,z) will not differ from the situation, which was valid one period $1/\nu_t$ (ν_t is the repetition rate of bunch trains) before, i.e. $T(t, x, y, z) = T(t - 1/\nu_t, x, y, z)$.
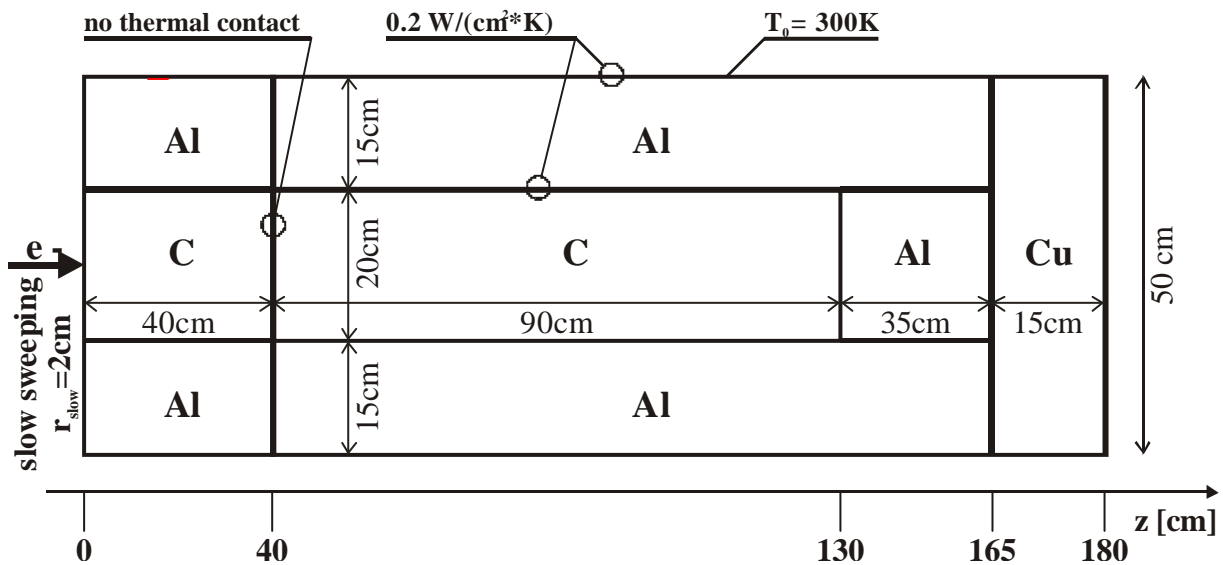

Figure 5.1: Geometry of variant A as used for the ANSYS calculations. Although shown here, the copper part was not included in the calculations.
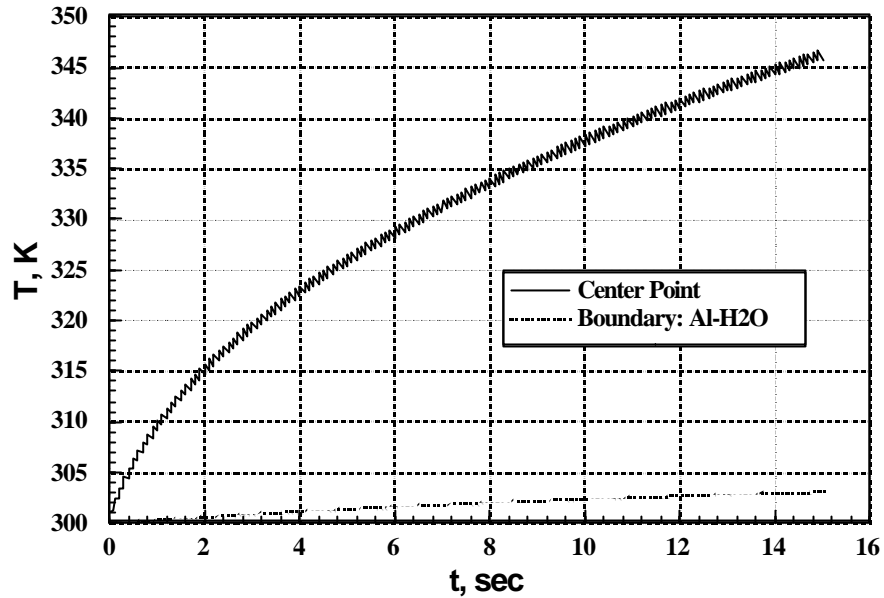
11

Figure 5.2: Development of temperature as function of time in the aluminum section at z=130cm, starting when the "cold" dump (300K) is exposed to beam.
Solid line at the center of the aluminum section r=0cm and dotted line near the circumference at r=25cm.

In that case steady state is reached. All calculated temperatures in the figures presented in this section are valid for steady state situation just after the passage of a bunch train. This is the time at which the maximum values of the temperatures can be expected. Since the temperature of the heat sink is explicitly specified with T_0=300K, all values given here are absolute temperatures T and not temperature differences relative to the heat sink.

In contrast to the rough and conservative estimation of heating in section 3, the temperature dependence of the heat capacity and heat conductivity of graphite and aluminum, as specified in table 5.1 and 5.2, are included. Specific heat of both materials and the thermal conductivity of

T [K]	300	400	500	700	1000	1500	2000	2500
l [W/(m⋅K)]	114	92	75	70	55	43	37	33
T [K]	300	400	500	800	1000	1200	1600	2000
c [J/(kg⋅K)]	678	1002	1233	1534	1800	1907	2036	2108

Table 5.1: Thermal conductivity and specific heat of graphite as a function of temperature

T [K]	300	600	900
l [W/(m⋅K)]	170	191	231
T [K]	250	400	600
c [J/(kg⋅K)]	861	948	1041

Table 5.2: Thermal conductivity and specific heat of aluminum as a function of temperature

	Graphite	Aluminum
r [g/cm^3]	1.71	2,7
E [N/m^2]	$1.1 \cdot 10^{10}$	$6.85 \cdot 10^{10}$
a [K^{-1}]	$7.3 \cdot 10^{-6}$	$2.6 \cdot 10^{-5}$

Table 5.3: Mechanical properties of graphite and aluminum (mass density ρ, elastic modulus E and coefficient of linear thermal expansion α).

aluminum grow with temperature, whereas graphite's thermal conductivity decreases at higher temperatures. The mechanical properties, like elastic modulus E, linear thermal expansion coefficient α and the mass density ρ, as used for the calculations are listed in table 5.3. Instead of pure radial heat flow, as assumed in section 3, ANSYS of course considers the fully 3-d solution of the heat equation. Therefore thermal diffusion within the bunch train passage time is included as well and will decrease instantaneous heating a little. In terms of average heating the problem is azimuthally symmetric, since the sweep circle is concentric to the dump axis, but each bunch train hits at another position along this circle. Therefore azimuthal symmetry is broken. Longitudinal heat flow will take place as well, but to be realistic, no thermal contact is assumed, where the 40cm extension part is attached to the existing TTF1 dump. Therefore a discontinuity can be observed in the temperature and stress profiles at this boundary. The heat transfer coefficient at the boundaries at r=10cm between the graphite respectively aluminum core and the surrounding aluminum as well as between dump surface and cooling water is specified to be $0.2 W/(cm^2 \cdot K)$ [5].

On this basis the temperature profiles shown in figures 5.3 to 5.6 are obtained. According to figure 5.3 and 5.5, the maximum temperature in the graphite section is about 650K≈380°C and 520K≈250°C in the downstream aluminum section. The highest temperature of the aluminum cylinder (see figure 5.6) is about 390K≈120°C at its inner radius (r=10cm) near z=0.6m. These results show, that the absorber will operate safely in terms of the tolerable temperatures in graphite and aluminum.

Looking at equilibrium heating, we know, that the maximum temperature only depends on the maximum power deposition $(dP/dz)_{max}$. From simple EMS parametrization formulae [6], one can derive, that $(dP/dz)_{max}$ is kept constant, if the average power P_{ave} varies with the beam energy E_0 in the following way:

$$P_{ave}(E_0) \propto \sqrt{\ln(E_0/E_c) - 0.37} \qquad \text{for} \quad (dP/dz)_{max} = \text{const}$$

E_c is the critical energy of the material, e.g. 76MeV for graphite. This relation tells, that the average beam power, even if it would be technically possible, can not stay at 130kW if the beam energy is less than 2GeV. Otherwise the dump would run in overload with respect to equilibrium heating. Table 5.4 shows this limit of the average power as a function of beam energy E_0. If TTF2

E_0 [GeV]	0.4	0.8	1.2	1.6	2.0
$\dfrac{P_{ave}(E_0)}{P_{ave}(2GeV)}$	67 %	83 %	91 %	96 %	100 %

Table 5.4: Average beam power as a function of beam energy E_0 if the maximum power deposition $(dP/dz)_{max}$, which determines equilibrium heating of the dump, is kept constant.

runs at 800MeV instead of 2GeV, the limit of the average power at the dump is 108kW according to this table. Although this operation is not possible with the given TTF2 parameters, since it would either exceed the bunch train population of $4 \cdot 10^{13}$ e- or the repetition rate of 10Hz, it should be pointed out, that the absorber is not capable of 130kW at lower beam energies. However if the maximum beam current of 64μA is not exceeded, the maximum average beam power achievable in TTF2 just scales with beam energy E_0 and is therefore below the tolerable absorber limit at any value of $E_0 \leq 2GeV$.

With the knowledge of the temperature profile ANSYS can also calculate the mechanical stress field in terms of the components σ_x, σ_y, σ_z. Difference between them is important for the estimation

of the resulting stress as a consequence of the heating. For a safe dump operation the equivalent stress σ_e must not exceed the tolerable strength $\sigma_{tolerable}$ of the material, that means:

$$\sigma_e = \frac{1}{\sqrt{2}} \cdot \sqrt{\left(\sigma_x - \sigma_y\right)^2 + \left(\sigma_x - \sigma_z\right)^2 + \left(\sigma_y - \sigma_z\right)^2} \leq \sigma_{tolerable}$$

Figure 5.7 shows the equivalent stress distribution in the dump of variant A. A closer look at the situation in the graphite core is given in figure 5.8.

Maximum equivalent stress in the graphite section is observed at the shower maximum at $z \approx 60$cm on the axis of the graphite core at r=0cm and near its boundary to the aluminum at r=10cm. A third maximum can be detected around $z \approx 20$cm and r=2cm. This is where instantaneous heating has its maximum, as we already know from figure 3.3. In absolute numbers the maximum equivalent stress in graphite is about 800N/cm^2, which is mainly determined by compression forces. This has to be compared to the tolerable compression strength of 9000N/cm^2 and the tolerable tension strength of 3000N/cm^2 for graphite. Therefore the graphite meets the required mechanical strength in the dump core.

Maximum stresses in the aluminum occur in the aluminum cylinder around z=80-100cm at its inner boundary to graphite and at its circumference. A small maximum is also located on the axis of the aluminum section downstream of the graphite core. In all these positions the equivalent stress is about 7000N/cm^2. The aluminum alloy used in the dump construction have a fluidity stress not less than 10000-13000N/cm^2, so that safe operation is guaranteed with a sufficient margin.

Summary

On the basis of using the existing 800MeV/50kW TTF1 dump, three realistic modifications were presented, which could be used as a beam dump for 2GeV/130kW TTF2 operation. The preferred solution consists of a 40cm front part extension, which has to be attached in front of the TTF1 dump and has the same radial graphite-aluminum geometry as the TTF1 dump. In addition a slow beam sweeping with a sweep radius of 2cm is required to reduce mainly the equilibrium heating of the graphite core.

As shown by temperature and mechanical stress calculations using the ANSYS code, this solution can safely deal with 800µs long bunch trains, which are populated with $4 \cdot 10^{13}$ electrons of 2GeV and repeat at 10Hz. The average beam power is therefore 130kW. The lower limit for the beam size, when entering the dump, is $\sigma_x \cdot \sigma_y = 1$mm^2. Otherwise systems to increase the spot size within the bunch train passage time, e.g. a fast sweeping system, have to be added.

Maximum temperatures in the aluminum part do not exceed 250°C. The dump can be operated at normal atmosphere. A special enclosure to prevent oxidization of the graphite is obsolete, since temperatures in the graphite do not exceed 400°C.
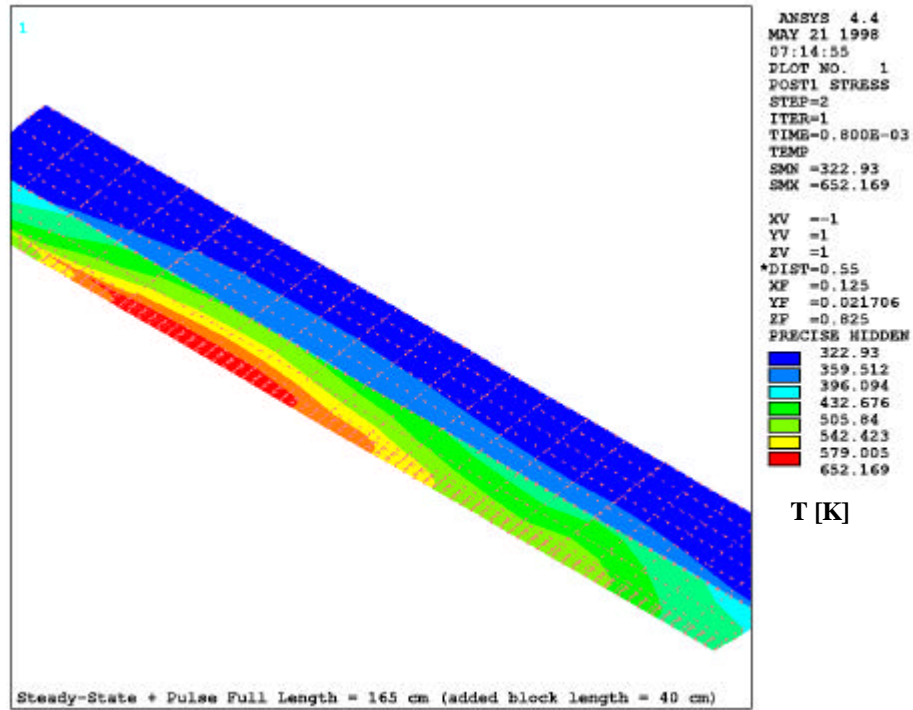
Figure 5.3: Absolute temperature distribution T(r,z) in units of Kelvin in the dump of variant A (0<r<25cm, 0<z<165cm), as calculated by ANSYS in steady state right after the passage of a bunch train.
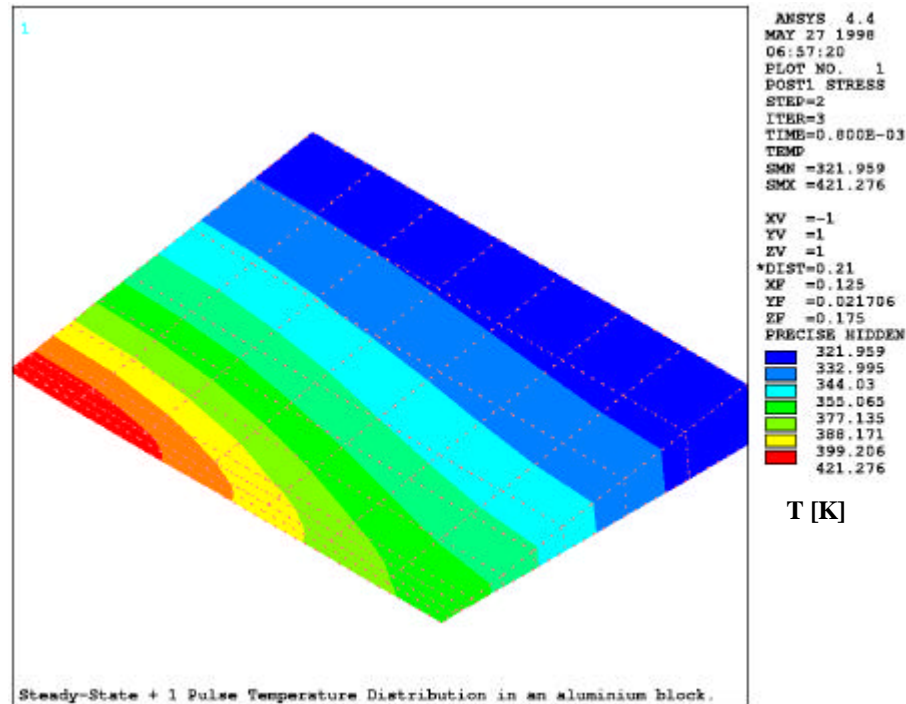

Figure 5.4: Absolute temperature distribution T(r,z) in units of Kelvin in the aluminum section (0<r<25cm, 130<z<165cm) downstream of the graphite section, as calculated by ANSYS in steady state right after the passage of a bunch train.
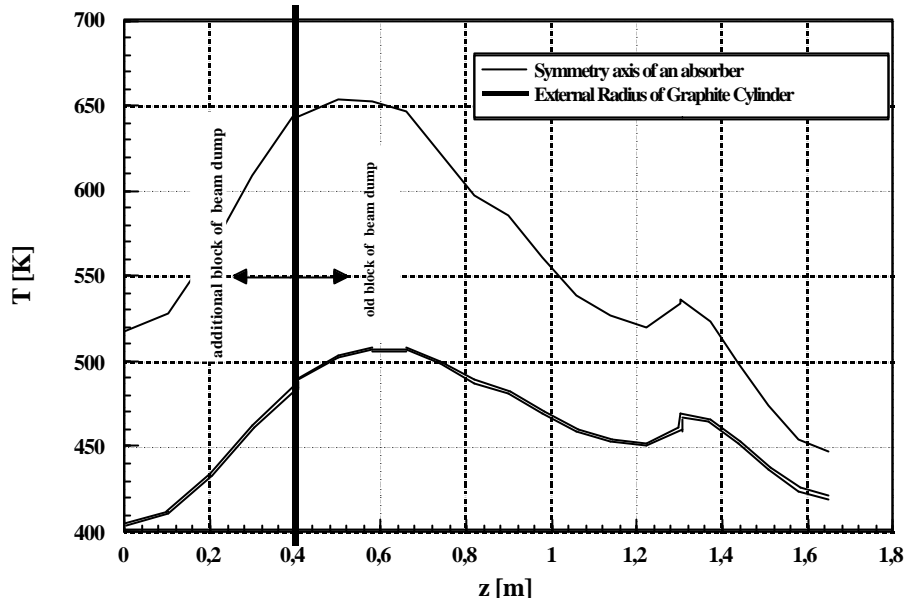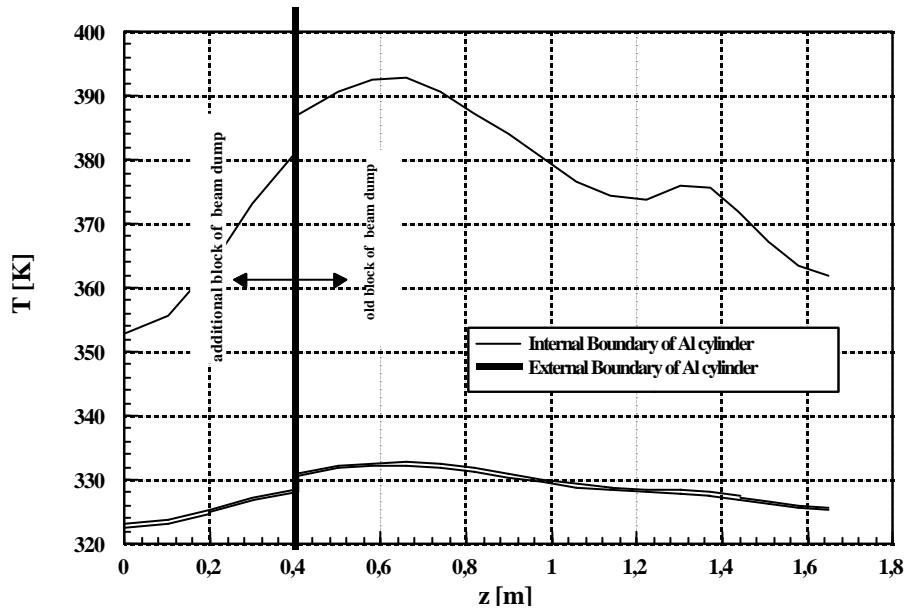
Figure 5.5: Absolute temperature profile T(r,z) in units of Kelvin in the dump of variant A along z, as calculated by ANSYS in steady state right after the passage of a bunch train.
Single solid line at r=2cm (max. energy deposition at sweep radius).
Double solid line at r=10cm (at the graphite side of the C-Al boundary).

Figure 5.6: Absolute temperature profile T(r,z) in units of Kelvin in the dump of variant A along z, as calculated by ANSYS in steady state right after the passage of a bunch train.
Single solid line at r=10cm (at the aluminum side of the C-Al boundary).
Double solid line at r=25cm (at the aluminum side of the Al-water cooling boundary).

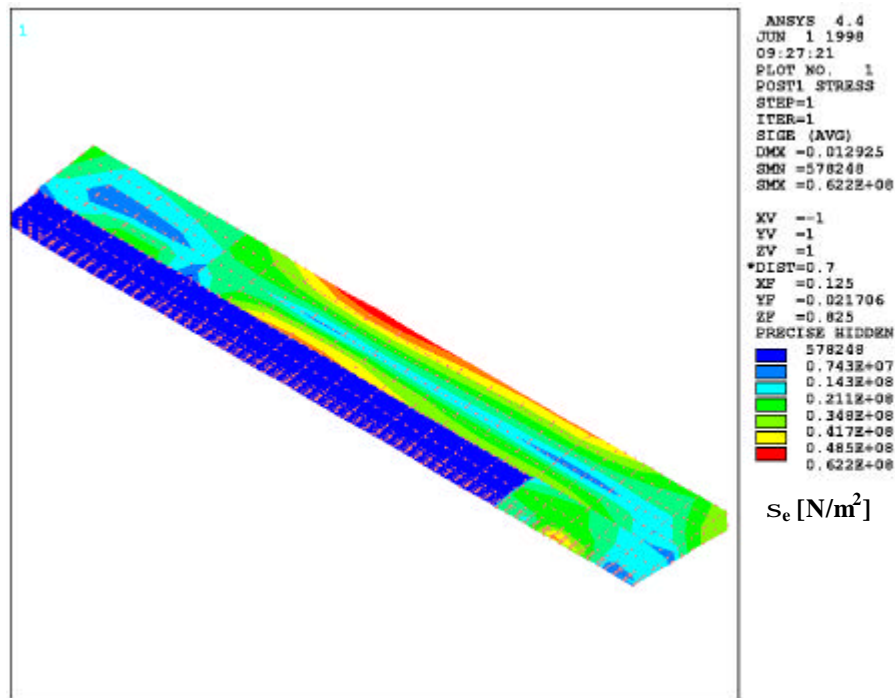*Figure 5.7:* Equivalent stress σ_e in units of N/m^2 in the dump of variant A, as induced by the temperature profile in steady state right after the passage of a bunch train.
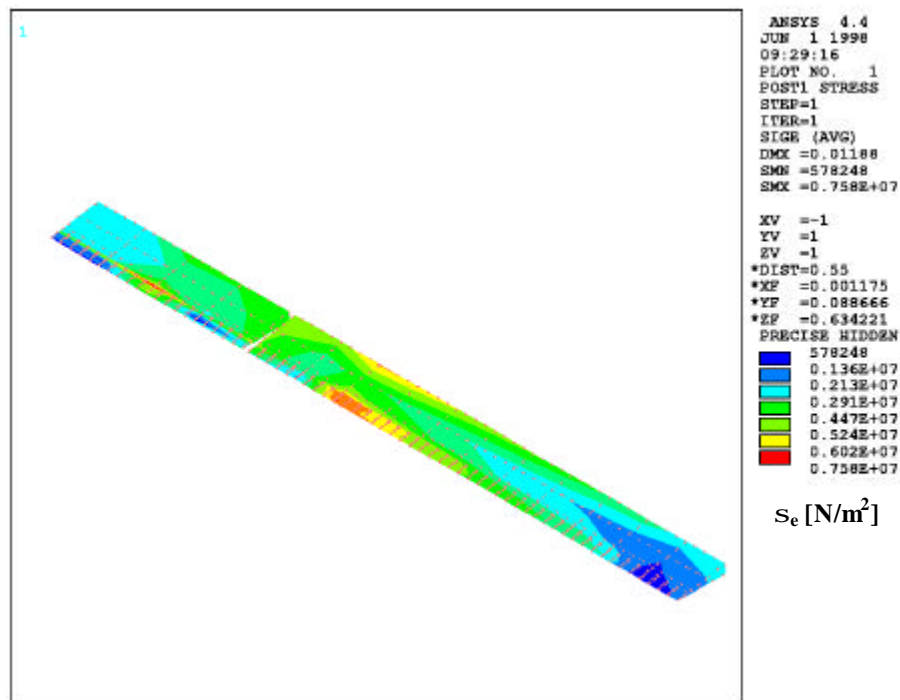

Figure 5.8: Equivalent stress σ_e in units of N/m^2 in the graphite core of the dump of variant A, as induced by the temperature profile in steady state right after the passage of a bunch train.

References

[1]   I.S. Baishev, M.A. Maslov, M. Seidel, Design of a Beam Dump for the TESLA
      and S-Band Test Facilities at DESY, DESY, May 1995, TESLA 95-10

[2]   N. V. Mokhov, The MARS Code System User's Guide, Version~13(95)''},
      Fermilab-FN-628 (1995),
      N. V. Mokhov et al., Fermilab-Conf-98/379 (1998),
      http://www-ap.fnal.gov/MARS/

[3]   ANSYS, User Manual, Awenson Analysis Systems Inc. (1983)

[4]   G. Grindhammer et al., The fast Estimation of Electromagnetic Showers,
      NIM A290 pages 469-488, 1990

[5]   J. Kidd et al., A high Intensity Beam Dump for the Tevatron Abort System,
      PAC IX, Washington, 1981

[6]   B. Rossi, High-Energy Particles, Prentice-Hall, New York, 1952